Evidence for a Broad Relativistic Iron Line from the Neutron Star LMXB Ser X-1

Sudip Bhattacharyya[1,2], and Tod E. Strohmayer[3]

ABSTRACT

We report on an analysis of *XMM-Newton* data from the neutron star low mass X-ray binary (LMXB) Serpens X-1 (Ser X-1). Spectral analysis of EPIC PN data indicates that the previously known broad iron Kα emission line in this source has a significantly skewed structure with a moderately extended red wing. The asymmetric shape of the line is well described with the `laor` and `diskline` models in XSPEC, which strongly supports an inner accretion disk origin of the line. To our knowledge this is the first strong evidence for a relativistic line in a neutron star LMXB. This finding suggests that the broad lines seen in other neutron star LMXBs likely originate from the inner disk as well. Detailed study of such lines opens up a new way to probe neutron star parameters and their strong gravitational fields. The `laor` model describes the line from Ser X-1 somewhat better than `diskline`, and suggests that the inner accretion disk radius is less than $6GM/c^2$. This is consistent with the weak magnetic fields of LMXBs, and may point towards a high compactness and rapid spin of the neutron star. Finally, the inferred source inclination angle in the approximate range 50°-60° is consistent with the lack of dipping from Ser X-1.

Subject headings: accretion, accretion disks — line: profiles — relativity — stars: neutron — X-rays: binaries — X-rays: individual (Ser X-1)

1. Introduction

The bright persistent LMXB Ser X-1 was discovered in 1965 (Bowyer et al. 1965). The detection of type I (thermonuclear) X-ray bursts from this source established that it

[1]CRESST and X-ray Astrophysics Lab, Astrophysics Science Division, NASA's Goddard Space Flight Center, Greenbelt, MD 20771; sudip@milkyway.gsfc.nasa.gov

[2]Department of Astronomy, University of Maryland, College Park, MD 20742

[3]X-ray Astrophysics Lab, Astrophysics Science Division, NASA's Goddard Space Flight Center, Greenbelt, MD 20771; stroh@clarence.gsfc.nasa.gov

harbors a neutron star (Swank et al. 1976; Li et al. 1977), as such bursts originate from the thermonuclear burning of matter accumulated on the surfaces of accreting neutron stars (Woosley & Taam 1976; Lamb & Lamb 1978; Strohmayer & Bildsten 2006). The lack of energy dependent dips and eclipses in the X-ray light curve of Ser X-1 suggests that its inclination angle may be less than 60° (Frank et al 1987; White & Swank 1982). The analysis of *RXTE* and *BeppoSAX* data revealed that the continuum spectra could be well fitted with a combination of absorbed Comptonization and disk blackbody models (Oosterbroek et al. 2001). Moreover, these authors reported the existence of a broad iron emission line near 6 keV, which they could adequately fit with a Gaussian model.

Broad iron emission lines (near 6 keV) have been observed from many LMXBs (Asai et al. 2000; Bhattacharyya et al. 2006; Miller et al. 2002a), and active galactic nuclei (AGN; Reynolds & Nowak 2003). These lines could be broadened by either Doppler and relativistic effects (due to Keplerian motion in the inner accretion disk; Fabian et al. 1989), or Compton scattering (in a disk corona; Misra & Kembhavi 1998). It has also been suggested recently that complex absorption from perhaps several ionized components may partially account for some of the broad line component (e.g., Turner et al. 2005). The *ASCA* data from the Seyfert-1 galaxy MCG-6-30-15 gave the first strong clues that such lines originate in the inner accretion disk, as the high signal-to-noise ratio data revealed a skewed and double-horned profile, consistent with Doppler, special relativistic, and general relativistic effects in the inner accretion disk, where the speed of matter is a substantial fraction of the speed of light (Tanaka et al. 1995). Analysis of recent data has strongly supported this inner disk origin of the line for MCG-6-30-15 and other AGN (Reynolds & Nowak 2003; Wilms et al. 2001; Reynolds et al. 2004; Reeves et al. 2007; Miniutti et al. 2007). Such lines, therefore, are extremely useful probes of strong gravity, and black hole properties, including spin (Brenneman & Reynolds 2006).

An inner disk origin has also been suggested for broad lines in some stellar mass black hole binaries, such as Cyg X-1 and GRS 1650–500 (Miller et al. 2002a; 2002b; Fabian et al. 1989). But, the origin of the broad iron lines from neutron star LMXBs has not been as well understood. This is largely because the available data had modest signal-to-noise ratio, and was not precise enough to rule out simple symmetric profiles (such as a Gaussian profile).

If the inner accretion disk origin can be established for broad iron lines from neutron star LMXBs, then the shape and width of the line may be used to constrain the radius of the inner edge of the disk, as well as the Keplerian speed at that radius. The former can give an upper limit to the neutron star radius (as the disk inner edge radius must be greater than or equal to the stellar radius), while both quantities may be utilized to constrain the stellar mass. Moreover, high frequency quasi-periodic oscillations (kHz QPOs) are observed from

many neutron star LMXBs (van der Klis 2006). Although the actual physical mechanism responsible for these timing features is still debated, the leading models involve strong gravity, with the accretion disk close to the neutron star surface. Therefore, if the inner disk origin can be established, the broad iron lines can be useful to constrain kHz QPO models, and together these two spectral and timing features will be extremely important as probes of strong gravity, and to constrain neutron star parameters. We note that the constraints on neutron star mass and radius can be useful to understand the nature of the high density cold matter at the stellar core, which is a fundamental problem of physics (see Bhattacharyya et al. 2005).

In this Letter, we present evidence for an inner accretion disk origin of the broad iron emission line in the X-ray spectrum of the neutron star LMXB Ser X-1. In § 2, we describe our analysis of *XMM-Newton* data, and in § 3 we discuss the implications of our results.

2. Spectral Analysis

The neutron star LMXB Ser X-1 was observed with *XMM-Newton* in March, 2004 three times (obsIds: 0084020401, 0084020501, 0084020601). These observations were separated in time by two days each, and each observation consists of about 22 ks of data. There are no European Photon Imaging Camera (EPIC) MOS detector data available for this source. EPIC PN observed the source in timing mode, and the source photons were also registered by the Reflection Grating Spectrometer (RGS) instruments. However, as no significant source spectral lines were detected in the RGS energy range, here we report only the analysis of the EPIC PN spectra.

We have excluded the portions of the EPIC PN data with high and variable background (due to soft proton flares), and extracted source spectra, background spectra, and response matrices using the *XMM-Newton* Science Analysis Software (SAS; version 3.0). The SAS task 'epatplot' has indicated that this set of spectra (set 1) is modestly piled up. We have, therefore, extracted another set of spectra (set 2) after excluding the contributions from the central (and hence the brightest) pixels in order to minimize the pile-up effect. Results from the two spectral sets are consistent with each other, and the broad double-peaked line, which is the focus of this Letter, is present in both sets in the same energy range. This is expected, as pile-up cannot generate a double-peaked line. Based on these findings we do not believe pile-up is a significant concern for our study. Therefore, we have used spectral set 1 because of its higher signal-to-noise ratio.

We have fitted the spectra with various models (within XSPEC), and found that the best

model to describe the observed continuum spectra consists of an absorbed Comptonization (compTT) component plus a disk blackbody (diskbb). The addition of diskbb to the compTT component is essential, as can be seen from Table 1. This is in accordance with observations of Ser X-1 obtained with other X-ray missions (see Oosterbroek et al. 2001). However, Oosterbroek et al. noted that the choice between a disk blackbody and a single temperature blackbody was arbitrary. But, our spectral fitting shows that a disk blackbody is preferred to a simple blackbody. For example, the choice of the former reduces the χ^2 by 76.6 compared to that for the latter (obs. 1, i.e., obsId 0084020401). Such a decrease in χ^2 is quite significant, and a similar decrease is found for obs. 2 (obsId 0084020501) and obs. 3 (obsId 0084020601). Table 1 shows that the addition of a Gaussian emission line near 0.54 keV improves the fit very significantly. As we have not found any source spectral lines at this energy in the RGS data, we suspect that this feature may be of instrumental origin, so we have fixed the line centroid of this feature at $\approx$ 0.54 keV in our subsequent model fitting. Finally, we have found highly significant excess emission near 6 keV. As a broad iron emission line is detected near this energy from many LMXBs (see § 1), we have fitted this excess emission with a Gaussian. This extra component is very significant (see Table 1), consistent with the results reported in Oosterbroek et al. (2001). However, as we have mentioned in § 1, it is not yet known with any certainty what broadens this line for neutron star LMXBs.

To explore this question in more detail we have replaced the 6 keV Gaussian component with the diskline model component of XSPEC. This component represents the spectral line emission from the inner portion of the accretion disk in the Schwarzschild spacetime (Fabian et al. 1989). The corresponding fits show that the diskline model describes the line profile significantly better than the simple Gaussian profile (see Table 1). This result supports the notion that the line is produced in the inner accretion disk. In order to further substantiate this result, we have also modeled the spectrum using the laor model. This model is similar to the diskline model, but it includes the effects of the spin of the central star (Laor 1991). The fact that the laor model also fits the line profile significantly better than the simple Gaussian (see Table 1) provides strong evidence of the inner disk origin of this line. In fact, laor describes the line somewhat better than diskline, as the choice of the former reduces the χ^2 by about 26 compared to that for the latter (obs. 1, i.e., obsId 0084020401). This suggests that the spin of the central star may have some effect on the line profile, by decreasing the disk inner edge radius (Laor 1991). Indeed, while the best-fit parameter values (including the continuum parameters) for the diskline component and the laor component are generally very consistent with each other, the best-fit inner disk radius ($R_{\rm in}$) for the latter model is smaller than that for the former. Here, we note that $R_{\rm in} \geq 6r_{\rm g}$ for diskline ($r_{\rm g} = GM/c^2$; M = central star mass).

In Table 2, we give the best-fit parameter values for the XSPEC model wabs*(compTT+

`diskbb+gauss+laor`) for each observation. These values do not change much from one obsId to another. We find the source inclination angle parameter ($i_{\rm L}$) in the range $\approx 50^\circ - 60^\circ$, which is consistent with the expected value ($< 60^\circ$; see § 1) for Ser X-1 (due to lack of eclipses and dips).

Fig. 1 shows the data, model components, and data-to-model ratio for observation 1. The `laor` model component for the broad iron line is clearly shown by the double-peaked dotted line. The moderately structured shape of the data-to-model ratio caused a relatively high reduced χ^2 for Ser X-1 (Table 2). Note that such structures and high reduced χ^2 were also reported by Oosterbroek et al. (2001; see their Figs. 5 & 6). These authors argued that these narrow structures could not be caused by an incorrect continuum modeling, since such incorrectness would probably give more smoothly varying data-to-model ratios.

We have added one more figure (Fig. 2) to show the structure of the broad relativistic iron line. The two panels show this line from two observations. The data points of the figure clearly show the line with an extended red wing. This figure also explicitly shows that both the `laor` model and the `diskline` model (dotted line in each panel) fit the spectral line profile well.

3. Discussion and Conclusions

In this Letter, we report the results of spectral fitting of the *XMM-Newton* EPIC PN data from the neutron star LMXB Ser X-1. The best-fit continuum parameter values (see Table 2) are generally consistent with those of Oosterbroek et al. (2001). Our slightly higher Comptonization plasma temperature ($T_{\rm C}$) compared to that of Oosterbroek et al. can be explained in terms of the lower $2 - 10$ keV flux that we have found. This is because, as the intensity of an LMXB decreases, its energy spectrum generally becomes harder.

It was previously known that Ser X-1 exhibits a broad iron line (see § 1), but earlier data did not have the statistical quality to rule out simple symmetric profiles (such as a Gaussian). As a result, its origin was not strongly constrained. Knowledge of the line's origin is very important, because if it is produced in the inner accretion disk, it can be used (1) to probe the strong gravitational field of the neutron star, (2) to constrain the stellar parameters, and (3) to constrain models of the kHz QPOs, which may, in turn, be useful to achieve the first two goals (see § 1). By analysing the *XMM-Newton* EPIC PN data we have demonstrated that the line is significantly asymmetric, and can be accurately modeled with physical models of line formation in the inner disk (using the `diskline` and `laor` models in XSPEC; see Fig. 2). This strongly supports the idea that this spectral line originates

from the inner accretion disk of Ser X-1 (see § 1). The high signal-to-noise ratio data also revealed the detailed shape of the broad and relativistically skewed line with an extended red wing (Fig. 2). Such lines have so far been observed from AGN and a few galactic black hole X-ray binaries (Tanaka et al. 1995; Miniutti et al. 2007; Miller et al. 2002a; 2002b), but this is the first strong evidence for a relativistic line in a neutron star system. As we have mentioned in § 1, other neutron star LMXBs exhibit broad iron emission lines, which so far have been adequately modeled with simple Gaussian profiles. Our finding for Ser X-1 suggests that the lines seen in other LMXBs may also originate from the inner accretion disk, and its relativistically skewed nature could be confirmed with sufficiently long observations. If future observations bear this out it will open up an exciting new opportunity to probe neutron stars and strong gravity with deep spectroscopic observations.

The best-fit line energies ($E_{\rm L}$) shown in Table 2 should be the result of the gravitational redshift of one of the Kα spectral lines (in the rest energy range $6.40-6.97$ keV) from neutral or ionized iron. The required redshift values are consistent with the radial range defined by the parameters $R_{\rm in}$ and $R_{\rm out}$ of the `laor` model component (see Table 2). This also suggests (from $R_{\rm in}$) that the accretion disk extends almost to the neutron star surface. This is not unexpected given the relatively low neutron star magnetic field in LMXBs ($\approx 10^{8-9}$ G), and the high accretion rate implied for Ser X-1 ($\approx 0.28\dot{M}_{\rm Edd} - 0.32\dot{M}_{\rm Edd}$; based on the observed flux, and the Eddington luminosity $\approx (2.0 - 3.8) \times 10^{38}$ ergs s^{-1} (distance $\approx 9.5 - 12.7$ kpc); Jonker & Nelemans 2004). In fact, the best-fit model suggests that the accretion disk may extend inside $6r_{\rm g}$ (although the 90% confidence range of $R_{\rm in}$ includes $6r_{\rm g}$; see Table 2), which is possible only if the neutron star is rather compact, and spins fast. However, we note that if the spin rate is too high, then depending on the stellar compactness and equation of state, the increased stellar equatorial radius may stop the disk outside $6r_{\rm g}$ (see Fig. 1 of Bhattacharyya et al. 2000). We have found that the equivalent width ($EW_{\rm L}$) of the iron line is lower than that reported in Oosterbroek et al. (2001), which may suggest that the strength of this line decreases with the source intensity. The source inclination angle inferred from each of `diskline` and `laor` fits is consistent with $\lesssim 60°$, whcih is expected for the non-dipping nature of Ser X-1 (see § 1).

Finally, the observed broad relativistic iron line is expected to be accompanied by a continuum reflection spectral component (Reynolds & Nowak 2003). A distinct feature of this component is a broad hump near 30 keV. As the signal-to-noise ratio of the EPIC PN data is small at higher energies ($\gtrsim 10$ keV), we could not determine if this component is present in the Ser X-1 spectra.

The authors thank Tim Kallman and Jean Cottam for helpful discussions. This work was supported in part by NASA Guest Investigator grants.

REFERENCES

Asai, K., Dotani, T., Nagase, F., & Mitsuda, K. 2000, ApJSS, 131, 571

Bhattacharyya, S., Strohmayer, T. E., Swank, J. H., & Markwardt, C. B. 2006, ApJ, 652, 603

Bhattacharyya, S., Strohmayer, T. E., Miller, M. C., & Markwardt, C. B. 2005, ApJ, 619, 483

Bhattacharyya, S., Thampan, A. V., Misra, R., & Datta, B. 2000, ApJ, 542, 473

Bowyer, S., Byram, E. T., Chubb, T. A., & Friedman, H. 1965, Science, 147, 394

Brenneman, L. W., & Reynolds, C. S. 2006, ApJ, 652, 1028

Fabian, A. C., Rees, M. J., Stella, L., & White, N. E. 1989, MNRAS, 238, 729

Frank, J., King, A. R., & Lasota, J.-P. 1987, A&A, 178, 137

Jonker, P. G., & Nelemans, G. 2004, MNRAS, 354, 355

Lamb, D. Q., & Lamb, F. K. 1978, ApJ, 220, 291

Laor, A. 1991, ApJ, 376, 90

Li, F. K. et al. 1977, MNRAS, 179, 21

Miller, J. M. et al. 2002a, ApJ, 578, 348

Miller, J. M. et al. 2002b, ApJ, 570, L69

Miniutti, G. et al. 2007, PASJ, 59, S315

Misra, R., & Kembhavi, A. K. 1998, ApJ, 499, 205

Oosterbroek, T., Barret, D., Guainazzi, M., & Ford, E. C. 2001, A&A, 366, 138

Reeves, J. N. et al. 2007, PASJ, 59, 301

Reynolds, C. S., & Nowak, M. A. 2003, Physics Reports, 377, 389

Reynolds, C. S., Wilms, J., Begelman, M. C., Staubert, R., & Kendziorra, E. 2004, MNRAS, 349, 1153

Strohmayer, T. E., & Bildsten, L. 2006, in *Compact Stellar X-ray Sources*, Eds. W.H.G. Lewin and M. van der Klis, (Cambridge University Press: Cambridge), 113

Swank, J. H., Becker, R. H., Pravdo, S. H., & Serlemitsos, P. J. 1976, IAU Circ., 2963

Tanaka, Y. et al. 1995, Nature, 375, 659

Turner, T. J., Kraemer, S. B., George, I. M., Reeves, J. N., & Bottorff, M. C. 2005, ApJ, 618, 155

van der Klis, M. 2006, in *Compact Stellar X-ray Sources*, Eds. W.H.G. Lewin and M. van der Klis, (Cambridge University Press: Cambridge), 39

White, N. E., & Swank, J. H. 1982, ApJ, 253, L61

Wilms, J. et al. 2001, MNRAS, 328, L27

Woosley, S. E., & Taam, R. E. 1976, Nature, 263, 101

Table 1. Fitting of the *XMM-Newton* EPIC PN energy spectra from Ser X-1 with various models of XSPEC.

No.	XSPEC Model	χ^2/dof[a] (Obs. 1[b])	χ^2/dof[a] (Obs. 2[b])	χ^2/dof[a] (Obs. 3[b])
1	`wabs*compTT`	$\frac{4581.8}{2287}$	$\frac{4121.2}{2230}$	$\frac{4250.6}{2256}$
2	`wabs*(compTT+diskbb)`	$\frac{3440.9}{2285}$ (0)	$\frac{2691.2}{2228}$ (0)	$\frac{3056.0}{2254}$ (0)
3	`wabs*(compTT+diskbb+gauss)`	$\frac{3238.7}{2283}$ (9.4E-31)	$\frac{2588.1}{2226}$ (1.3E-19)	$\frac{2947.0}{2252}$ (1.8E-18)
4	`wabs*(compTT+diskbb+gauss+gauss)`	$\frac{2917.4}{2280}$ (2.3E-51)	$\frac{2411.5}{2223}$ (7.6E-34)	$\frac{2689.8}{2249}$ (2.8E-44)
5	`wabs*(compTT+diskbb+gauss+diskline)`	$\frac{2843.0}{2277}$ (1.0E-12)	$\frac{2379.8}{2220}$ (1.8E-6)	$\frac{2644.0}{2246}$ (2.2E-8)
6	`wabs*(compTT+diskbb+gauss+laor)`	$\frac{2817.2}{2277}$ (3.6E-17)	$\frac{2373.0}{2220}$ (8.5E-8)	$\frac{2633.6}{2246}$ (2.8E-10)

[a]The number in the parentheses is the probability (calculated from F-test using XSPEC) of the decrease of χ^2/dof by chance from the value of the previous row to the that of the current row (for models $2-5$). For model 6, the comparison is with model 4. A very small value is replaced with a zero.

[b]Obs. 1: ObsId 0084020401; Obs. 2: ObsId 0084020501; Obs. 3: ObsId 0084020601.

Table 2. Best fit parameters (with 90% confidence) for the *XMM-Newton* EPIC PN energy spectra from Ser X-1.

Parameter[a]	Obs. 1[b]	Obs. 2[b]	Obs. 3[b]
$N_{\rm H}$[c] (10^{22} atoms cm^{-2})	$0.48^{+0.03}_{-0.01}$	$0.45^{+0.01}_{-0.01}$	$0.47^{+0.03}_{-0.02}$
T_0[d] (keV)	$0.18^{+0.01}_{-0.01}$	$0.19^{+0.01}_{-0.01}$	$0.18^{+0.02}_{-0.02}$
$T_{\rm C}$[e] (keV)	$3.22^{+0.32}_{-0.09}$	$2.69^{+0.15}_{-0.04}$	$3.00^{+0.25}_{-0.18}$
$\tau_{\rm C}$[f]	$6.22^{+0.13}_{-0.32}$	$7.12^{+0.20}_{-0.37}$	$6.53^{+0.37}_{-0.47}$
$T_{\rm in}$[g] (keV)	$1.67^{+0.04}_{-0.02}$	$1.22^{+0.04}_{-0.03}$	$1.42^{+0.06}_{-0.05}$
$E_{\rm L}$[h] (keV)	$5.99^{+0.05}_{-0.05}$	$6.07^{+0.07}_{-0.05}$	$6.12^{+0.04}_{-0.05}$
$\beta_{\rm L}$[i]	$1.52^{+0.40}_{-0.17}$	$1.29^{+0.32}_{-0.26}$	$0.88^{+0.26}_{-0.64}$
$R_{\rm in}$[j]	$2.61^{+3.71}_{-1.38}$	$2.05^{+7.39}_{-0.82}$	$2.61^{+6.86}_{-1.38}$
$R_{\rm out}$[k]	$47.6^{+7.3}_{-3.2}$	$78.6^{+22.4}_{-11.4}$	$61.1^{+3.9}_{-7.0}$
$i_{\rm L}$[l] (degree)	$57.3^{+1.8}_{-2.0}$	$59.6^{+3.72}_{-2.15}$	$54.6^{+2.0}_{-1.8}$
$EW_{\rm L}$[m](eV)	$130.6^{+8.0}_{-8.1}$	$122.1^{+16.8}_{-14.6}$	$118.9^{+13.4}_{-13.1}$
χ^2/dof	2817.2/2277	2373.0/2220	2633.6/2246
Flux[n] ($0.5-2$ keV)	0.93	0.87	0.91
Flux[n] ($2-10$ keV)	4.22	3.34	3.79

[a]Parameters of the XSPEC model `wabs*(compTT+diskbb+gauss+laor)`.

[b]Obs. 1: ObsId 0084020401; Obs. 2: ObsId 0084020501; Obs. 3: ObsId 0084020601.

[c]Hydrogen column density from the `wabs` model component.

[d]Input soft photon (Wien) temperature of the `compTT` model component.

[e]Temperature of the Comptonizing plasma (`compTT` model component).

[f]Optical depth of the Comptonizing plasma (`compTT` model component).

[g]Temperature at inner disk radius from `diskbb` model component.

[h]Energy of the broad relativistic iron emission line (`laor` model component).

[i]Power law index of emissivity (`laor` model component).

[j]Inner radius (in the unit of GM/c^2; M is the mass of the neutron star) from the `laor` model component.

[k]Outer radius (in the unit of GM/c^2) from the `laor` model component.

[l]Source inclination angle from the `laor` model component.

[m]Equivalent width of the broad relativistic iron emission line (`laor` model component).

[n]Flux in 10^{-9} ergs cm^{-2} s^{-1}.

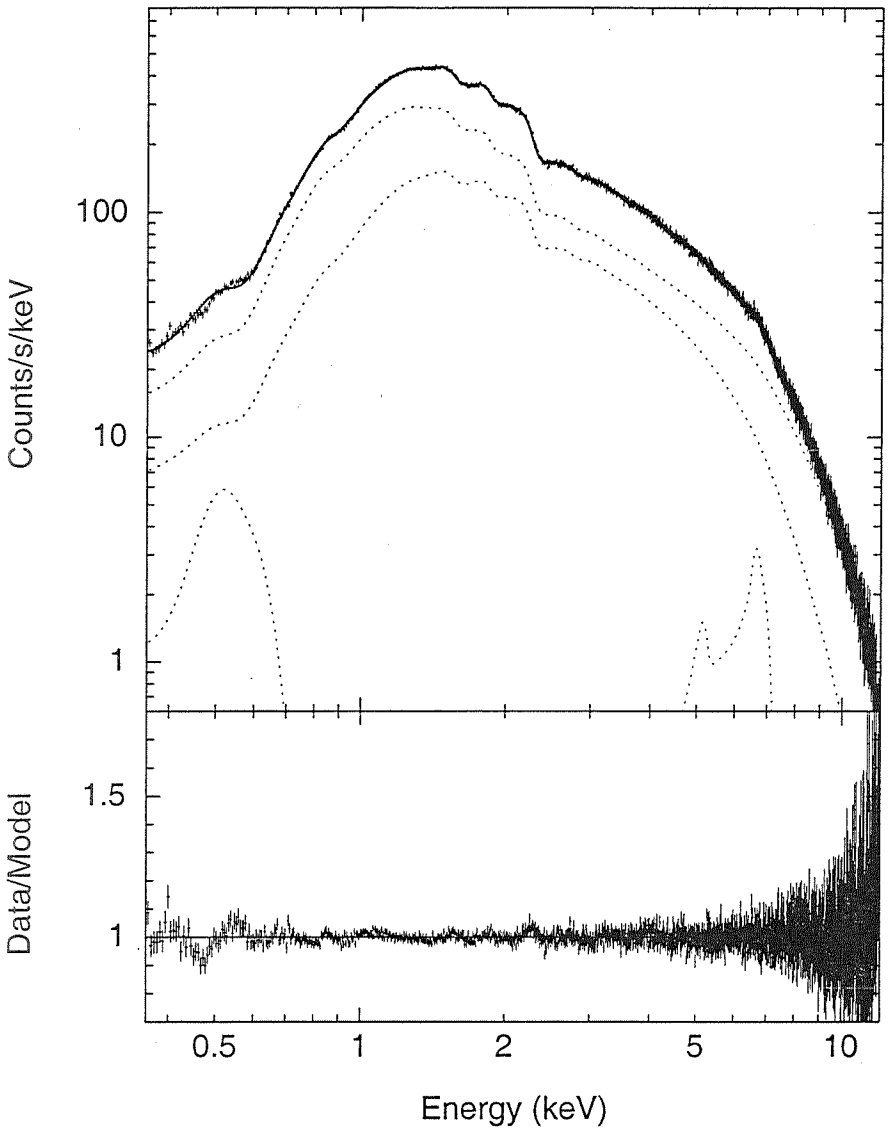

Fig. 1.— *XMM-Newton* EPIC PN energy spectrum from Ser X-1 for obs. 1 (obsId 0084020401). The upper panel shows the data (error bars), model (solid line), and individual additive model components (dotted lines). Here we have used the best-fit XSPEC model `wabs*(compTT+diskbb+gauss+laor)` (see Table 2). Among the two continuum additive model components, the upper dotted line shows `compTT`, and the lower dotted line shows `diskbb`. The low energy emission line is the `gauss` component, while the high energy broad iron emission line is the `laor` component. The lower panel shows the data to model ratio. This figure shows that the iron line is double-peaked, and hence relativistic.

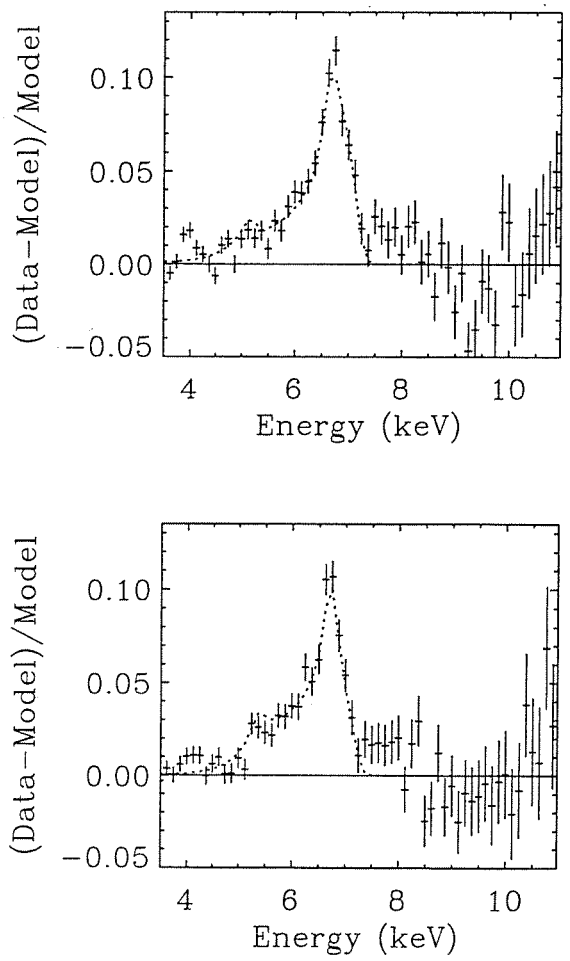

Fig. 2.— *Upper panel*: *XMM-Newton* EPIC PN energy spectrum from Ser X-1 for obs. 1 (obsId 0084020401). With the error bars we show the data intensity in excess of the model intensity, and normalized by the model intensity (i.e., (Data−Model)/Model). Here the model is the best-fit model (of Table 2) minus the `laor` component. The `laor` component is separately shown with the dotted line. *Lower panel*: Similar to the upper panel, but for obs. 3 (obsId 0084020601), and for the `diskline` component (model 5 of Table 1) instead of the `laor` component. For each panel, the data points clearly show a broad relativistic iron emission line with an extended red-wing. This line should have originated from the inner accretion disk, as both the `laor` model component, and the `diskline` component (of XSPEC) fit it well.